Avens Publishing Group
J Chem Applications
July 2026 Volume:6, Issue:1

Open Access Research Article

Journal of
Chemistry & Applications

Microwave-Assisted Green Fabrication of Gum Neem Capped Gold Nanoparticles for Efficient Catalytic Reduction

Banu R[1*] and Mohan KC[2]

[1]*Department of Chemistry, Dr. BRR GDC(A) Jadcherla, Mahabubnagar Telangana, India.*
[2]*Departmentof Chemistry, MALD Government Degree College Gadwal Telangana, India.*

***Address for Correspondence:**
Ruqya Banu, Department of Chemistry, Dr. BRR GDC(A) Jadcherla, Mahabubnagar Telangana, India. EMail Id: ruqyabrr@gmail.com

Submission: 20 June, 2026
Accepted: 19 August, 2026
Published: 22 August, 2026

Keywords: Gold Nanoparticles; Gum Neem; Green Synthesis; Catalytic Activity; UV–Vis Spectroscopy; Biogenic Nanoparticles.

Abstract

A simple and environmentally friendly method was developed for the green synthesis of stable gold nanoparticles (AuNPs) using Gum Neem (GN) as both the reducing and capping agent. The synthesized AuNPs were characterized by UV–Vis spectroscopy, Fourier-transform infrared (FTIR) spectroscopy, X-ray diffraction (XRD), and Transmission electron microscopy (TEM). The UV–Vis spectrum exhibited a characteristic surface plasmon resonance (SPR) band at 520–550 nm, confirming the formation of AuNPs. FTIR analysis revealed that the hydroxyl (–OH) functional groups present in Gum Neem played a crucial role in the reduction of tetrachloroauric acid to metallic gold nanoparticles. XRD analysis confirmed the crystalline nature of the nanoparticles with a face-centered cubic (fcc) structure, while TEM images showed uniformly dispersed, nearly spherical nanoparticles with an average particle size of 12 ± 4 nm. The biosynthesized AuNPs exhibited excellent catalytic activity toward the reduction of hexacyanoferrate(III) in the presence of sodium borohydride ($NaBH_4$). The reaction progress was monitored by UV–Vis spectroscopy, and the catalytic efficiency of the AuNPs was evaluated through kinetic studies by varying the reaction temperature and catalyst concentration.

Introduction

In recent years, noble metal nanoparticles, particularly gold (Au), silver (Ag), and platinum (Pt), have attracted significant research interest because of their unique physicochemical properties at the nanoscale, which differ considerably from those of their bulk counterparts. These properties can be precisely tailored by controlling the size, shape, and morphology of the nanoparticles, making them highly suitable for a broad range of technological and biomedical applications.

Among noble metal nanomaterials, gold nanoparticles (AuNPs) have emerged as one of the most extensively investigated owing to their exceptional optical, electronic, catalytic, and biocompatible properties. Their size-dependent characteristics have enabled applications in catalysis, chemical and biological sensing, electronics, drug delivery, disease diagnosis, and other biomedical fields. In particular, AuNPs have demonstrated remarkable catalytic efficiency in electron-transfer and hydrogenation reactions, making them promising catalysts for various industrial and environmental applications [1].

Recently, biomass-derived materials have emerged as attractive renewable resources for sustainable nanotechnology. Natural biomass sources, including medicinal plants, agricultural wastes, natural polymers, and other biological materials, are rich in bioactive constituents such as polyphenols, flavonoids, alkaloids, proteins, carbohydrates, and organic acids. These compounds act as both reducing and stabilizing agents during the synthesis of metal nanoparticles. Compared with conventional chemical methods, biomass-mediated synthesis offers several advantages, including eco-friendliness, cost-effectiveness, enhanced biocompatibility, improved nanoparticle stability, and long-term sustainability. As a result, biomass-derived nanomaterials have gained significant attention for applications in catalysis, environmental remediation, sensing, energy storage, antimicrobial and antioxidant therapies, and drug delivery [2–6].

The catalytic performance of colloidal AuNPs is commonly evaluated using model reduction reactions, such as the reduction of hexacyanoferrate(III) to hexacyanoferrate(II). This reaction is widely employed because it can be conveniently monitored by UV–Vis spectroscopy, and the reduction proceeds at an appreciable rate only in the presence of an efficient catalyst. Consequently, this model reaction provides a reliable approach for evaluating the catalytic activity and reaction kinetics of metal nanoparticles. Similar catalytic studies have also been reported for platinum and silver nanoparticles.

Conventionally, gold nanoparticles have been synthesized using various physical and chemical methods, including chemical reduction, photochemical synthesis, electrochemical reduction, thermal evaporation, and laser-assisted techniques. Although these methods produce nanoparticles with well-controlled characteristics, they often require expensive instrumentation, harsh reaction conditions, and hazardous reducing or stabilizing agents such as sodium borohydride, hydrazine, sodium citrate, and other synthetic chemicals. The use of these toxic reagents raises concerns regarding environmental pollution and biological safety.

ISSN: 2380-5021

To overcome these limitations, green synthesis has emerged as a sustainable and environmentally benign alternative for nanoparticle production. Green synthetic approaches utilize naturally occurring biomolecules from plant extracts, polysaccharides, natural gums, microorganisms, and other renewable resources as reducing and stabilizing agents, thereby eliminating the need for toxic chemicals. These methods are simple, cost-effective, biocompatible, and eco-friendly while producing stable nanoparticles with excellent functional properties. Consequently, green synthesis has become an attractive strategy for developing gold nanoparticles for catalytic, biomedical, and environmental applications.

To promote sustainable nanotechnology, researchers have increasingly focused on biological systems as environmentally friendly alternatives for nanoparticle synthesis. Various biological resources, including plants, bacteria, fungi, viruses, algae, agricultural waste, and natural biopolymers, have been successfully employed as reducing and stabilizing agents for the green synthesis of metal nanoparticles. Among these, plant-derived natural gums have received considerable attention because they are renewable, biodegradable, non-toxic, and readily available. Moreover, nanoparticle synthesis using these gums is typically carried out in aqueous media under mild reaction conditions, eliminating the need for hazardous chemicals and making the process economical and environmentally friendly. Several studies have reported the successful synthesis of gold nanoparticles using natural gums such as gum katira, kondagogu gum, and gellan gum, in which the biomolecules act as both reducing and capping agents [7].

Gum Neem (GN), a natural exudate obtained from the stems and branches of *Azadirachta indica*, is a complex polysaccharide containing limonoids and other bioactive constituents. Owing to its excellent biocompatibility, non-toxic nature, water solubility, and film-forming ability, Gum Neem has been widely used as a stabilizer, emulsifier, binder, and coating material in the food, pharmaceutical, and cosmetic industries. The abundance of hydroxyl and other functional groups in its molecular structure enables Gum Neem to effectively reduce metal ions while simultaneously preventing nanoparticle aggregation. Previous studies have demonstrated its successful application in the green synthesis of silver and palladium nanoparticles.

Motivated by these advantages, the present study explores the use of Gum Neem as a dual-function reducing and stabilizing agent for the eco-friendly synthesis of gold nanoparticles. The synthesized AuNPs were comprehensively characterized using UV–Vis spectroscopy, Fourier-transform infrared (FTIR) spectroscopy, X-ray diffraction (XRD), and transmission electron microscopy (TEM). Furthermore, the catalytic performance of the biosynthesized AuNPs was evaluated through the electron-transfer reduction of hexacyanoferrate(III) to hexacyanoferrate(II) in the presence of sodium borohydride. The reaction kinetics were systematically investigated by UV–Vis spectroscopy to assess the catalytic efficiency of the synthesized nanoparticles.

Biosynthesis “of Gold nanoparticles employing Gum Neem extract and their potential application as” Catalytic Reduction.

Experimental

Materials

Chloroauric acid trihydrate ($HAuCl_4 \cdot 3H_2O$, 99.9%) was obtained from Sigma-Aldrich. Gum Neem (laboratory reagent grade, spray-dried), sodium borohydride ($NaBH_4$), potassium hexacyanoferrate(III), and sodium hydroxide (NaOH) were purchased from S. D. Fine Chemicals Ltd., Mumbai, India. All aqueous solutions were prepared using double-distilled water, and all chemicals were used as received without further purification.

Green Synthesis of Gum Neem-Capped Gold Nanoparticles (GN-AuNPs)

Gold nanoparticles (AuNPs) were synthesized using Gum Neem as both the reducing and stabilizing agent. Initially, a 1% (w/v) Gum Neem stock solution was prepared by dissolving the required amount of Gum Neem powder in double-distilled water under continuous magnetic stirring for 1 h at room temperature until a homogeneous solution was obtained.

For the synthesis of AuNPs, 3 mL of the Gum Neem solution was mixed with 1 mL of 1 mM chloroauric acid ($HAuCl_4$) solution in a clean boiling tube. The reaction mixture was subjected to microwave irradiation for 5 min. The formation of AuNPs was confirmed by a distinct color change from pale yellow to ruby red, indicating the reduction of Au^{3+} ions to metallic gold nanoparticles.

To optimize the synthesis conditions, the concentrations of Gum Neem (0.1–1.0%, w/v) and chloroauric acid (0.1–1.0 mM) were systematically varied while maintaining all other reaction parameters constant. The synthesized nanoparticles were subsequently characterized using UV–V is spectroscopy, Fourier-transform infrared (FTIR) spectroscopy, X-ray diffraction (XRD), and transmission electron microscopy (TEM).

Characterization of Gold Nanoparticles

The optical properties of the synthesized AuNPs were investigated using a UV–Vis spectrophotometer (Shimadzu UV-3600) over the wavelength range of 200–700 nm to monitor the characteristic surface plasmon resonance (SPR) band.

FTIR spectroscopy was performed to identify the functional groups of Gum Neem involved in the reduction and stabilization of the nanoparticles. Prior to analysis, the colloidal AuNP suspension was freeze-dried, and the resulting powder was thoroughly mixed with potassium bromide (KBr) to prepare transparent pellets. A pure KBr pellet was used as the background reference. The FTIR spectra were recorded using a Shimadzu IRAffinity-1 spectrometer over the wavenumber range of 400–4000 cm^{-1}.

The crystalline structure of the synthesized AuNPs was analyzed

ISSN: 2380-5021

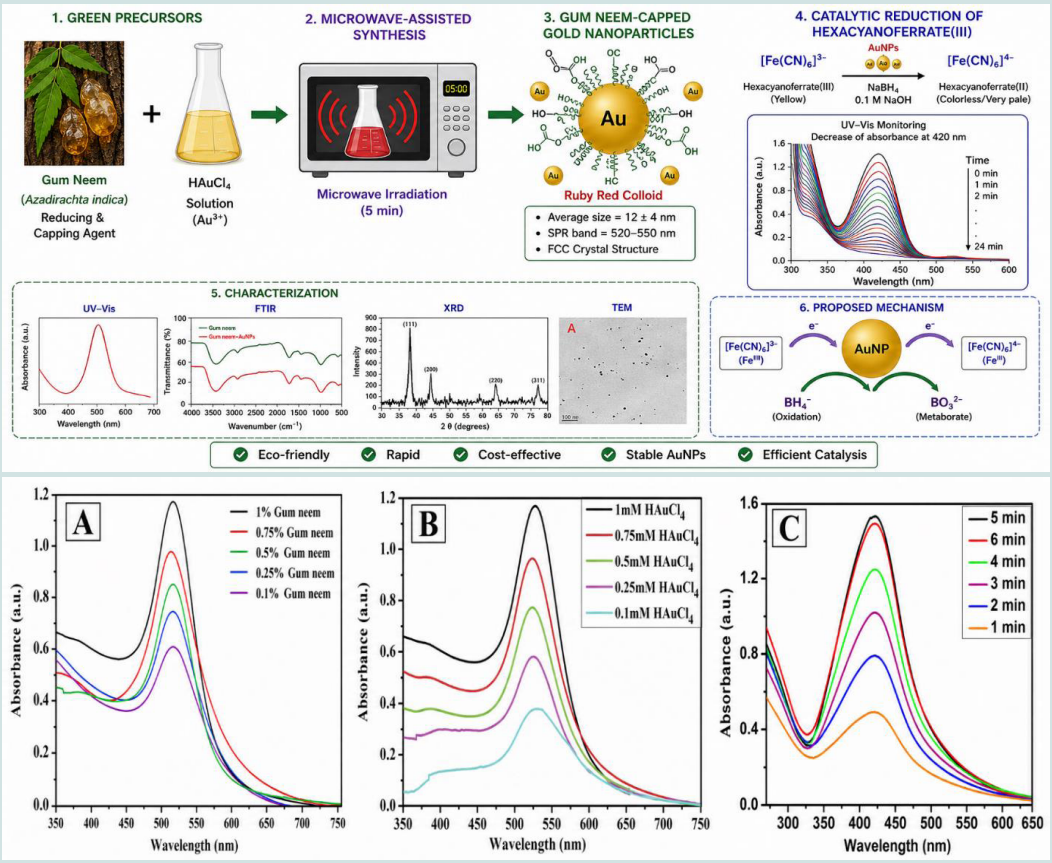

Figure 1: UV–V is absorption spectra of AuNPs synthesized using (A) different concentrations of Gum Neem, (B) different concentrations of $HAuCl_4$, and (C) different microwave irradiation times.

by X-ray diffraction using a Rigaku MiniFlex diffractometer equipped with Cu Kα radiation.

The morphology, particle size, and particle size distribution of the synthesized AuNPs were examined using transmission electron microscopy (JEOL JEM-2000 FX-II). For TEM analysis, a drop of the colloidal AuNP suspension was placed onto a carbon-coated copper grid and allowed to dry overnight at room temperature before imaging [8].

Catalytic Reduction of Hexacyanoferrate (III)

The catalytic activity of the synthesized AuNPs was evaluated through the electron-transfer reduction of potassium hexacyanoferrate(III) using sodium borohydride ($NaBH_4$) as the reducing agent. The reaction mixture was prepared by mixing 1.0 mL of double-distilled water, 0.5 mL of 10 mM aqueous potassium hexacyanoferrate(III) solution, and 1.5 mL of 36 mM sodium borohydride solution prepared in 0.1 M NaOH in a standard 3 mL quartz cuvette. Subsequently, the required amount of the AuNP catalyst was added to initiate the reaction.

The alkaline medium (0.1 M NaOH) was used to minimize the hydrolytic decomposition of sodium borohydride and to maintain its reducing capability throughout the experiment. The progress of the reaction was monitored using a UV–Vis spectrophotometer by recording the decrease in absorbance at 420 nm, corresponding to the reduction of hexacyanoferrate(III) to hexacyanoferrate(II).

To investigate the effect of temperature on the catalytic performance, the reduction reaction was carried out over the temperature range of 30–70 °C while maintaining constant reactant concentrations. The effect of catalyst loading was also evaluated by varying the volume of the AuNP suspension from 50 to 200 µL under otherwise identical reaction conditions.

Results and Discussion

UV–Vis Spectroscopy

UV–Vis spectroscopy is a simple, sensitive, and widely used technique for the characterization of noble metal nanoparticles. The formation and stabilization of gold nanoparticles (AuNPs) in aqueous solution were monitored by UV–Vis spectroscopy. The reduction of Au^{3+} ions to metallic Au^0 by Gum Neem was indicated by a distinct color change of the reaction mixture from pale yellow to ruby red. The characteristic surface plasmon resonance (SPR) absorption band of AuNPs was observed in the wavelength range of 520–550 nm .

ISSN: 2380-5021

(Figure 1A) shows the UV–V is spectra of AuNPs synthesized using 1 mM chloroauric acid and varying concentrations of Gum Neem (0.1–1.0%, w/v). As the Gum Neem concentration increased, the intensity of the SPR band increased, indicating enhanced formation of AuNPs.

(Figure 1B) illustrates the UV–Vis spectra obtained by varying the concentration of chloroauric acid (0.1–1.0 mM) while maintaining the Gum Neem concentration at 1% (w/v). The intensity of the SPR band increased with increasing $HAuCl_4$ concentration, confirming greater nanoparticle formation [9].

The effect of microwave irradiation time on AuNP synthesis was also investigated (Figure 1C). The reaction conditions were systematically optimized to achieve maximum nanoparticle yield and stability.

Fourier-Transform Infrared (FTIR) Spectroscopy

The FTIR spectra of Gum Neem-mediated gold nanoparticles confirmed the involvement of Gum Neem biomolecules in the reduction and stabilization of AuNPs. The broad absorption band observed at 3200–3500 cm^{-1}, corresponding to the O–H stretching vibration of polysaccharides, became broader and shifted slightly after nanoparticle formation, indicating the participation of hydroxyl groups in the reduction of Au^{3+} ions.

The absorption band at approximately 1600–1650 cm^{-1}, assigned to carbonyl (C=O) and carboxylate (COO^-) groups, also exhibited a slight shift, suggesting their interaction with the AuNP surface. Similarly, the characteristic C–O and C–O–C stretching vibrations in the region of 1000–1100 cm^{-1} showed changes in intensity and position after nanoparticle synthesis, confirming the adsorption of Gum Neem polysaccharides onto the nanoparticle surface. Minor spectral changes observed in the 1400–1450 cm^{-1} region further support the involvement of carboxylate groups in the capping process [10-12].

Overall, these spectral changes demonstrate that the hydroxyl, carbonyl, carboxyl, and ether functional groups present in Gum Neem act as both reducing and stabilizing agents during the synthesis of AuNPs.

X-ray Diffraction (XRD)

The crystalline structure of the synthesized AuNPs was investigated by X-ray diffraction (XRD). As shown in Figure 3, four distinct diffraction peaks were observed at 2θ values of 38.08°, 44.09°, 64.42°, and 77.39°, corresponding to the (111), (200), (220), and (311) crystallographic planes, respectively. These diffraction peaks are characteristic of the face-centered cubic (fcc) crystal structure of metallic gold and agree well with the standard reference data (JCPDS No. 04-0784).

The absence of additional diffraction peaks indicates the high purity of the synthesized nanoparticles, while the sharp diffraction peaks confirm their highly crystalline nature. The average crystallite size, calculated using the Debye–Scherrer equation from the full width at half maximum (FWHM) of the (111) reflection, was approximately 14 nm. This value agrees well with the particle size obtained from TEM analysis [13-15].

Transmission Electron Microscopy (TEM)

The morphology, particle size, and size distribution of the biosynthesized AuNPs were examined using transmission electron microscopy (TEM). Representative TEM micrographs of AuNPs synthesized using 1% Gum Neem and 1 mM $HAuCl_4$ after microwave

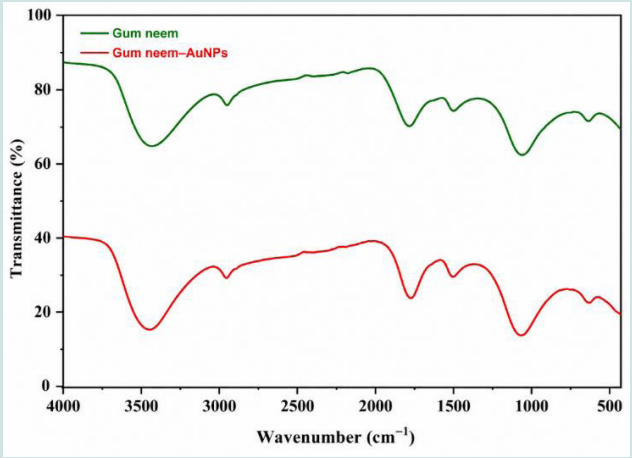

Figure 2: FTIR spectra of pure Gum Neem (GN) and Gum Neem-capped AuNPs.

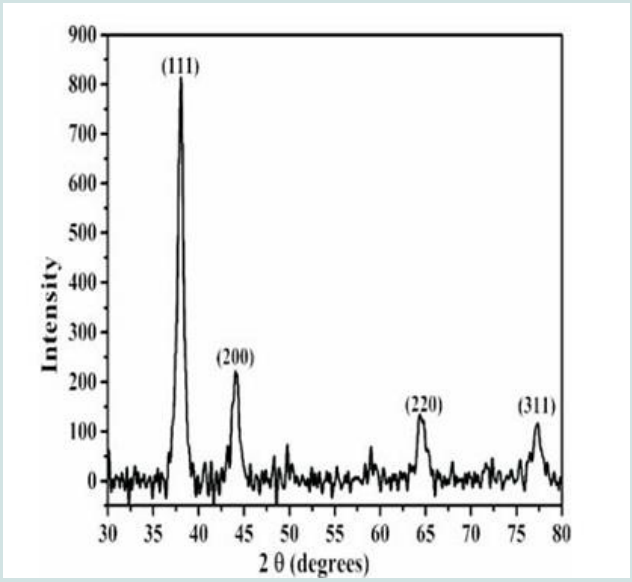

Figure 3: XRD pattern of Gum Neem-capped AuNPs synthesized using 1% (w/v) Gum Neem and 1 mM $HAuCl_4$ after microwave irradiation for 5 min.

ISSN: 2380-5021

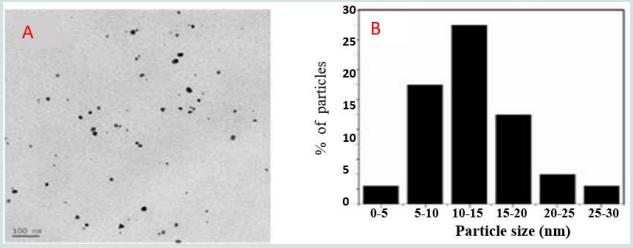

Figure 4: (A) TEM micrograph of Gum Neem-capped AuNPs and (B) the corresponding particle size distribution histogram.

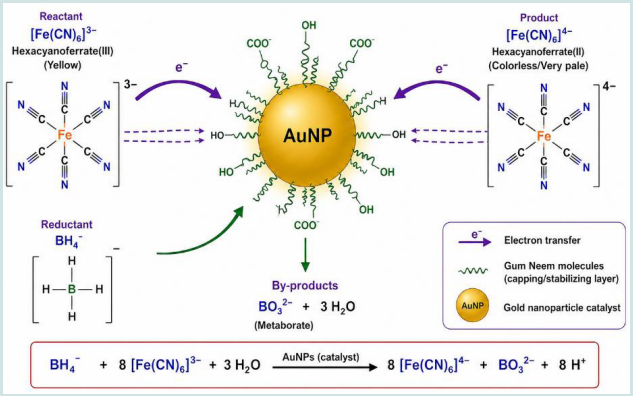

Figure 5: Proposed Mechanism of AuNPs Catalyzed Reductionof Hexacyanoferrate (III) by $NaBH_4$.

irradiation for 5 min are presented in (Figure 4A).

The TEM images revealed predominantly spherical nanoparticles with only a few irregularly shaped particles [16-18]. The nanoparticles were uniformly dispersed with minimal aggregation, indicating effective stabilization by Gum Neem. Analysis of individual nanoparticles showed an average particle size of **12 ± 4 nm**, as illustrated in the corresponding particle size distribution histogram (Figure 4B) [19-21].

Catalytic Reduction of Hexacyanoferrate(III)

The catalytic activity of the biosynthesized AuNPs was evaluated through the electron-transfer reduction of potassium hexacyanoferrate(III) by sodium borohydride ($NaBH_4$), producing hexacyanoferrate(II) and metaborate ions according to the following reaction:

Both Fe(III) and Fe(II) complexes are highly stable and possess similar coordination geometries. The standard reduction potential of the Fe(III)/Fe(II) redox couple is +0.44 V, whereas borohydride oxidation occurs at −1.24 V versus the normal hydrogen electrode. Although the reaction is thermodynamically favorable, it proceeds very slowly in the absence of a catalyst because of a significant kinetic barrier. Consequently, AuNPs act as efficient electron-transfer mediators, markedly accelerating the reduction reaction.

The reaction progress was monitored by UV–Vis spectroscopy. Potassium hexacyanoferrate(III) exhibits a characteristic absorption band at approximately 420 nm. Upon addition of AuNPs, the absorbance at 420 nm decreased progressively with reaction time, confirming the catalytic reduction of hexacyanoferrate(III) to hexacyanoferrate(II) (Figure 6A). Because sodium borohydride was present in large excess, the reaction followed pseudo-first-order kinetics with respect to hexacyanoferrate(III) .Throughout the reaction, the SPR band of the AuNPs at approximately 530 nm remained essentially unchanged, indicating excellent colloidal stability without aggregation. The absence of any significant shift or broadening of the SPR band further demonstrates that no undesirable interaction occurred between the reactants and the nanoparticle catalyst.

The effect of catalyst loading was investigated by varying the volume of AuNP suspension from 50 to 250 µL while maintaining constant concentrations of hexacyanoferrate (III), sodium borohydride, and temperature. The apparent rate constant increased linearly with increasing catalyst loading, indicating that a greater number of active surface sites enhanced electron transfer and accelerated the reduction reaction [22-25].

The influence of temperature was also examined over the range of 30–70 °C. As expected, the reaction rate increased with increasing temperature because of enhanced molecular collisions and faster electron-transfer kinetics. The activation energy (E_a) was determined using the Arrhenius equation by plotting ln(k) versus 1/T (Figure 6B). From the slope ($-E_a/R$), the activation energy was calculated to be **7.6 kcal mol^{-1}**, demonstrating that the biosynthesized AuNPs effectively lower the activation energy and facilitate rapid electron-transfer reactions.

Conclusion

A simple, rapid, and environmentally friendly microwave-assisted method was successfully developed for the green synthesis of gold nanoparticles using Gum Neem as both the reducing and stabilizing agent. The synthesized AuNPs exhibited a characteristic SPR band at approximately 520 nm. XRD and TEM analyses confirmed the formation of highly crystalline face-centered cubic (fcc) AuNPs

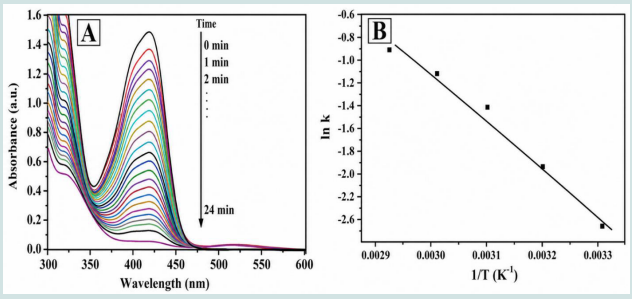

Figure 6: (A). Time-dependent UV-V is spectra of the mixture of hexacyanoferrate (III) and sodium borohy dride upon addition of gold nanoparticles (B) The pseudo First order kinetics of reduction4.

ISSN: 2380-5021

with an average particle size of 12 ± 4 nm, while FTIR spectroscopy demonstrated that hydroxyl and carboxyl functional groups were responsible for the reduction and stabilization of the nanoparticles. The synthesized AuNPs exhibited excellent catalytic activity toward the sodium borohydride-assisted reduction of hexacyanoferrate(III), following pseudo-first-order kinetics. Increasing the catalyst loading and reaction temperature significantly enhanced the reaction rate, demonstrating the potential of Gum Neem-mediated AuNPs as efficient, sustainable, and environmentally friendly nanocatalysts for catalytic applications.

Acknowledgement

The infrastructure facilities required to carry out the experiments were provided by Department of Chemistry Dr. B.R.R. Government Degree College(A), Jadcherla , for which the authors is grateful. Additionally, the authors would like to thank Prof. G. Sukanya, Principal of "Dr. B.R.R. Government Degree College, Jadcherla," to provide the essential facilities and support.

References

1. Daniel MC, Astruc D (2004) Gold nanoparticles: Assembly, supramolecular chemistry, quantum-size-related properties, and applications toward biology, catalysis, and nanotechnology. *Chem Rev* 104: 293-346.
2. Sushmitha S, Rao L, Nayak MP, Hegde SS, Bhat BR (2026) Clitoria ternatea-mediated ZnO nanoparticles for enzyme-free photoelectrochemical cholesterol detection. Materials Advances 7: 5768–5780.
3. Choudari BN, Hegde SS, Herbert MA, Kumar GN, Bhat BR (2026) Thermochemically activated Ficus benghalensis leaf-derived porous activated carbon for sustainable supercapacitor electrodes. RSC Advances 16: 11864-11873.
4. Ramarao, Desai BK, Basavanneppa MA, Narayanrao K, Pruthviraj N, Sharanagouda H, et al. (2026) Biogenic zinc oxide and silicon dioxide nanoparticles derived from spinach and paddy husk for enhanced rice cultivation. Discover Materials 6: 194.
5. Hugar AC, Hanagadakar MS, Hiremath JN, Raghu AV (2025) Antibacterial activity of Ag nanoparticles embedded in tragacanth gum-based composite hydrogel synthesized with acrylamide and 2-acrylamido-2-methylpropanesulfonic acid. Polymer Bulletin 82: 9821-9838.
6. Choudari BN, Hegde SS, Herbert MA, Kumar GN, Bhat BR (2026) Valorizing biomass into ultrahigh-surface-area porous carbon for sustainable next-generation energy storage. RSC Advances.
7. Dreaden EC, Alkilany AM, Huang X, Murphy CJ, El-Sayed MA (2012) The golden age: Gold nanoparticles for biomedicine. *Chem Soc Rev* 41: 2740–2779.
8. Philip D (2010) Green synthesis of gold and silver nanoparticles using Hibiscus rosa-sinensis. *Spectrochim Acta A Mol Biomol Spectrosc* 77: 807-810.
9. Song JY, Kim BS (2009) Rapid biological synthesis of gold nanoparticles using plant leaf extracts. *Bioprocess Biosyst Eng* 32: 79-84.
10. Shankar SS, Rai A, Ahmad A, Sastry M (2004) Rapid synthesis of Au, Ag and bimetallic nanoparticles using neem leaf broth. *J Colloid Interface Sci* 275: 496-502.
11. Ghosh P, Han G, De M, Kim CK, Rotello VM (2008) Gold nanoparticles in drug delivery. *Adv Drug Deliv Rev* 60: 1307-1315.
12. Rai M, Yadav A, Gade A (2008) Current trends in phytosynthesis of metal nanoparticles. *Crit Rev Biotechnol* 28: 277-284.
13. Thakkar KN, Mhatre SS, Parikh RY (2010) Biological synthesis of metallic nanoparticles. *Nanomedicine* 6: 257-262.
14. Li X, Xu H, Chen ZS, Chen G (2011) Biosynthesis of nanoparticles by microorganisms and their applications. *J Nanomater* 2011:1-16.
15. Hebbalalu D, Lalley J, Nadagouda MN, Varma RS (2013) Greener techniques for the synthesis of silver nanoparticles. *ACS Sustain Chem Eng* 1: 703-712.
16. Varma RS (2016) Journey on greener pathways: From the use of alternate energy inputs to sustainable applications. *ACS Sustain Chem Eng* 4: 5866-5878.
17. Polshettiwar V, Varma RS (2010) Green chemistry by microwave irradiation. *Green Chem* 12: 743-754.
18. Kharissova OV, Dias HVR, Kharisov BI, Pérez BO, Pérez VMJ (2013) The greener synthesis of nanoparticles. *TrAC Trends Anal Chem* 44: 47-61.
19. Shah M, Fawcett D, Sharma S, Tripathy SK, Poinern GEJ (2015) Green synthesis of metallic nanoparticles via biological entities. *Materials* 8: 7278-7308.
20. Anastas PT, Warner JC (2000) *Green Chemistry: Theory and Practice.* Oxford University Press.
21. Agarwal Dc (2013) Introduction to nanoscience and nanomaterials.
22. Kalpana VN, Devi Rajeswari V (2018) Green synthesis of gold nanoparticles using plant extracts and their catalytic applications. *Mater Today Proc.*
23. Irfan M, Moniruzzaman M (2021) Microwave-assisted green synthesis of gold nanoparticles: A review. *J Mol Liq.* 2021.
24. Li Y, Schluesener HJ, Xu S (2010) Gold nanoparticle-based biosensors. *Gold Bull* 43: 29-41.
25. Singh P, Kim YJ, Zhang D, Yang DC (2016) Biological synthesis of nanoparticles from plants and microorganisms. *Trends Biotechnol* 34: 588-599.